Journal of Luminescence 255 (2023) 119541

Contents lists available at ScienceDirect

Journal of Luminescence

journal homepage: www.elsevier.com/locate/jlumin

Full Length Article

High-temperature photoluminescence OF $CsPbBr_3$ perovskite nanocrystals in the fluorophosphate glasses

E.V. Kolobkova [a,b,*], R. Semaan [a], M.S. Kuznetsova [c], N.V. Nikonorov [a]

[a] ITMO University, Birzhevaya Line 4, St. Petersburg, 199034, Russia
[b] St. Petersburg State Institute of Technology (Technical University), Moskovsky pr. 26, St. Petersburg, 190013, Russia
[c] Spin Optics Laboratory, Saint Petersburg State University, 198504, St. Petersburg, Russia

ARTICLE INFO

Keywords:
$CsPbBr_3$ perovskites
Fluorophosphate glass
Nanocrystals
Quantum dot
Photoluminescence
Band gap shift

ABSTRACT

For the first time the temperature dependence of the photoluminescence of the semiconductor $CsPbBr_3$ perovskite nanocrystals with sizes of 6.0–9.0 nm in fluorophosphate glass were investigated in the temperature range from 300 K to 423 K. It was shown that temperature dependence of the photoluminescence intensity and the band gap shift coefficient change at 350 K corresponding to the isostructural phase transition. The photoluminescence intensity decreased radically above this temperature. The temperature energy gap coefficients of the $CsPbBr_3$ nanocrystals depending on the size and temperature range were found.

1. Introduction

The prospects of using Colloidal $CsPbX_3$ nanocrystals (NCs) are associated with a high quantum yield and high color purity of the luminescence [1,2], which makes these materials promising media for light-emitting devices, such as low-threshold lasers [3,4], light-emitting diodes (LEDs) [5–12] and semitransparent luminescent solar concentrators [13]. However, retention of these useful properties at high temperatures is one of the challenges when using such NCs in many optoelectronic technologies. It turned out that in real devices, the stability of optical characteristics at temperatures often exceeding 100 °C is required since these devices heat up during long-term operation. One of the possible approaches to the isolation of nanocrystals from the influence of the environment is their formation in a glassy matrix [14–18].

It was indicated that perovskite NCs in the glasses could be attractive luminescent materials for many applications due to their strong light absorption and high quantum yield (QY), which is close to QY magnitude of colloidal nanocrystals. However, there is practically no work on the analysis of the temperature influence on the NCs photoluminescence (PL) in glass. Only in Ref. [19] the PL properties of $CsPbBr_3$ perovskite quantum dots (QDs) with sizes of 6.6, 8.4 and 9.6 nm embedded in phosphate glasses were investigated in the temperature range of 40–240 K. PL integral intensities, band gap energies of $CsPbBr_3$ QDs showed a complicated dependences on temperature and sizes. The complex dependence, apparently, was associated with isostructural order-disorder phase transitions in the range of 160–180 K [20], which was not taken into account. Changes occurring with an increase of temperature above room temperature for NCs in glasses have not been previously considered. However, there are works in which the high temperature luminescence of bulk and colloidal nanocrystals is discussed [21–27]. The temperature changes of the absorption and PL spectra of $CsPbBr_3$ bulk crystals were studied in Ref. [21]. Analysis of the results showed that the value of temperature band gap shift coefficient dEg/dT was $\sim -0.8 \times 10^{-4}$ eV K^{-1} up to 380 K and increased to -3.41×10^{-4} eV K^{-1}at higher temperatures. The temperature of 380 K corresponds to the transition from the orthorhombic to the tetragonal phase, which is fixed by the X-ray diffraction (XRD). The sign of the temperature coefficient did not change during phase transitions. Thus, the changes in the crystal phase, recorded by XRD, exactly coincided with the change in the slope of the temperature band gap shift.

The changes of the band gap in colloidal $CsPbX_3$ (X = Cl, Br, I) NCs with an increasing temperature from 4 to 300 K were studied in Refs. [22–24]. In Ref. [25], changes in the band gap positions and PL loss pathways were reported with increasing temperature from 80 to 550 K. A constant temperature shift coefficient was observed over the entire temperature range, which indicates that the phase of colloidal NCs is unchanged up to 550 K, which is quite differ from bulk crystals [21]. In Ref. [25] were shown that i) PL loss pathways are mainly due to a thermally-assisted trapping, most likely to halogen vacancy traps; (ii) exciton separation is not, by itself, an explanation for decreased PL with

* Corresponding author. ITMO University, Birzhevaya Line 4, St. Petersburg, 199034, Russia.
E-mail address: kolobok106@rambler.ru (E.V. Kolobkova).

https://doi.org/10.1016/j.jlumin.2022.119541
Received 15 June 2022; Received in revised form 8 November 2022; Accepted 18 November 2022
Available online 28 November 2022

increasing temperature; (iii) reversible PL loss mechanisms (up to 450 K) are independent on the NCs size over the range 7–11 nm.

However, it was shown perovskite $CsPbBr_3$ NCs undergo a reversible, photoinduced phase transition as a result of high-power exposure [26]. $CsPbBr_3$ NCs was studied from 298 to 373 K [27] and it was found that the optical bandgap was independent on the temperature in this range. In Ref. [28] the PL spectrum excited by two-photon absorption showed a linear blue-shift ($3.2\ 10^{-4}$ eV K^{-1}) below the temperature of 220 K. For higher temperatures, the PL peak approaches a roughly constant value up to 380 K.

In our work, $CsPbBr_3$ perovskite NCs were formed in a new low-melting fluorophosphate glass (FP). The possibility of introducing of the high halides content in the FP glasses was a reason for choosing this type of glass matrix. Our previous research has shown the versatility of a FP glasses to create optical materials with unique properties due to developed synthesis technique that allowed us to keep controlled active components content in the glass. Lead and cadmium sulfoselenide QDs were synthesized in the FP glasses [29–32]. High luminescent and nonlinear optical characteristics were achieved due to higher QDs content than in the other glass host. In Ref. [33] we showed the features of the $CsPbX_3$ (X = Cl, Br, I) NCs formation in these glasses.

In the present study, we examine the optical properties of $CsPbBr_3$ NCs in FP glass in the high temperature range of 300–423 K using PL measurements.

2. Experimental procedures

2.1. Glassceramics preparation

Samples of FP glass with composition of $40P_2O_5$–35BaO–5NaF $10AlF_3$-$10Ga_2O_3$ (mol. %) - doped with Cs_2O, PbF_2 and $BaBr_2$ were synthesized using melt-quench technique.

The glass synthesis was performed in closed glassy carbon crucible at temperature T = 1000 °C. About 50 g of the batch was melted in a crucible for 30 min, then the glass melt was cast on a glassy carbon plate and pressed to form a plate with thickness ~2 mm. Samples with a diameter of 7–8 cm were annealed at a temperature of 50 °C below glass transition temperature (T_g = 400 °C).

$CsPbBr_3$ perovskite NCs were precipitated by the glass self-crystallization during melt-quenching and additional heat treatment at 400 °C. The initial glass doped with ~6 nm NCs was obtained by controlling of the residual concentration of bromine, and the cooling rate of the melt without heat treatment. The glasses doped with ~7.5 and ~9 nm NCs were obtained after heat treatment of the initial glass at 400 °C during 30 and 60 min, correspondingly.

2.2. Glass characterization

Differential scanning calorimeter STA 449F1 Jupiter Nietzsche was used for measurement of the glass transition temperature (T_g).

The precipitation of $CsPbBr_3$ NCs in FP glass was identified by X-ray diffraction. Cu-$_{K\alpha}$ irradiation (λ = 1.5406 Å) with a scanning rate of 2°/min was used for the measurement with resolution of 0.02° using a Rigaku X-ray diffractometer.

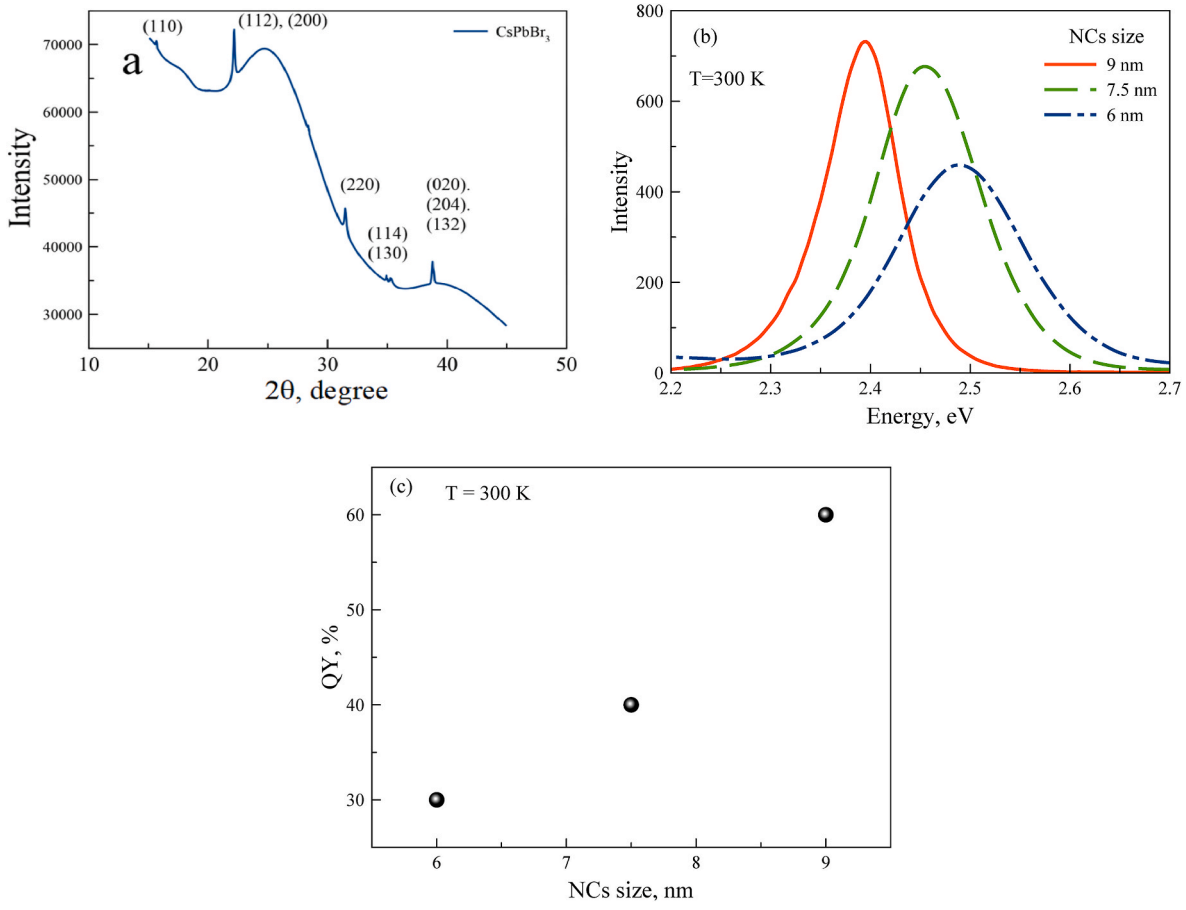

Fig. 1. (a) XRD spectra of the glass doped with NCs with size 11 nm (JCPDS No. 01-072- 7929): (b) PL and (c) quantum yield of FP glass containing $CsPbBr_3$ NCs with three different sizes (~6.0, 7.5, 9.0 nm) at room temperature.

The luminescence properties at room temperature were characterized using MPF-44A (PerkinElmer) spectrofluorimeter and Absolute PL Quantum Yield Measurement System (Hamamatsu). Temperature-dependent PL measurements were carried out in a Specac cryostat in the temperature range of 295–423 K with step of 10 K.

The absorption spectra of FP glass samples at room temperature were recorded in the 200–800 nm spectral region using Lambda 650 PerkinElmer spectrophotometer.

3. Results and discussion

Fig. 1a shows an XRD pattern of the FP glasses doped with $CsPbBr_3$ NCs confirming the formation nanocrystalline perovskite $CsPbBr_3$. The low concentration of NCs does not make it possible to accurately determine the perovskite phase because of intense peaks of the high and low temperature phases coincide. A decrease in NCs symmetry is realized in the appearance of additional low-intensity peaks and double main peaks. In Fig. 1a, the designations of the peaks are given for the orthorhombic phase (JCPDS No. 01-072- 7929).

A specific property of $CsPbBr_3$ bulk crystals and colloidal nanocrystals, which differs them from other semiconductors, is an unusual temperature dependence of the band gap. In most semiconductors, the band gap energy increases with decreasing temperature, however, $CsPbBr_3$ semiconductors show the opposite behavior, namely, the band gap energy increases with increasing temperature [21,24,25].

To analyze the temperature dependence of the PL and the band gap changes, we considered three glass samples doped with CsPbBr3 NCs of different sizes. PL bands with maxima at 2.49, 2.46 and 2.4 eV at room temperature were recorded (Fig. 1b). Such changes in the emission corresponded to a change in size from ~6 to 9 nm [19,33]. It should be noted that the PL maxima of the QDs formed in these samples actually coincided, judging by the positions of the PL bands, with those studied in phosphate glasses in Ref. [19]. Fig. 1c shows the Quantum Yield of FP glass containing $CsPbBr_3$ NCs with three different sizes (~6.0, 7.5, 9.0 nm) at room temperature.

Note that the Bohr exciton radius determining the range of size confinement for the CsPbBr3 is ~7.0 nm. Therefore, the 2R/aB ratio of the QDs studied in the present work was 0.85 —1.5 and NCs corresponds to the regime of so-called “medium quantum confinement” when the QDs size is near Bohr exciton radius of the bulk crystal.

In Figs. 2–4 are presented the results for three studied samples with different sizes 6, 7.5 and 9 nm. The PL spectra (a) and the inverse temperature dependences of the integral PL intensity (b) are presented with increasing temperature from 300 to 423 K. The inverse temperature dependences of the integrated intensity can be approximated by two straight lines with different slopes. An increase of the slope is observed at a temperature of ~350 K ($1/T = 0.285\ K^{-1}$). This temperature is close to the temperature of the first-order isostructural transition within the P_{21}/m space group of single crystals [20]. In Ref. [25] the mechanism of PL loss in $CsPbX_3$ NCs was identified as thermal electron occupation of halogen vacancy centers. The excellent luminescent properties of $CsPbBr_3$ NCs has been linked to halide vacancy tolerance arising from the shallow nature of halide vacancy states [34,35]. Nonetheless, these vacancies may be responsible for PL losses at higher temperatures [25]. An increase of the slope above 350 K might indicate a change in the luminescence quenching mechanism. We can to suggest that in addition to traditional temperature quenching, due to the growth of absorbing traps [25], an intensity decrease is triggered due to the transition of

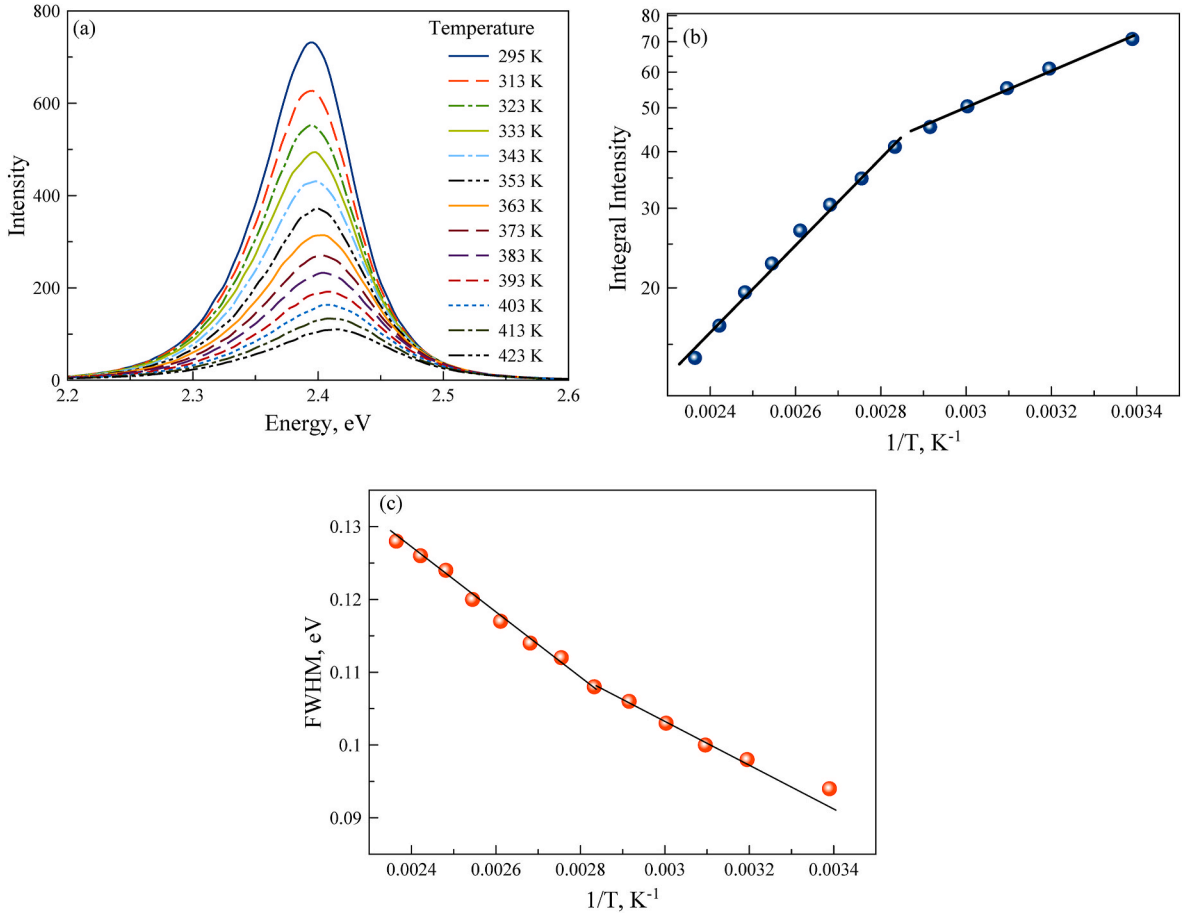

Fig. 2. PL spectra at different temperatures (a) and the dependence of PL integral intensity in logarithmic scale on the inverse temperature (b); and the inverse temperature dependence of PL FWHM (c) for NCs with an average size of 9 nm in FP glass during heating from 300 to 423 K.

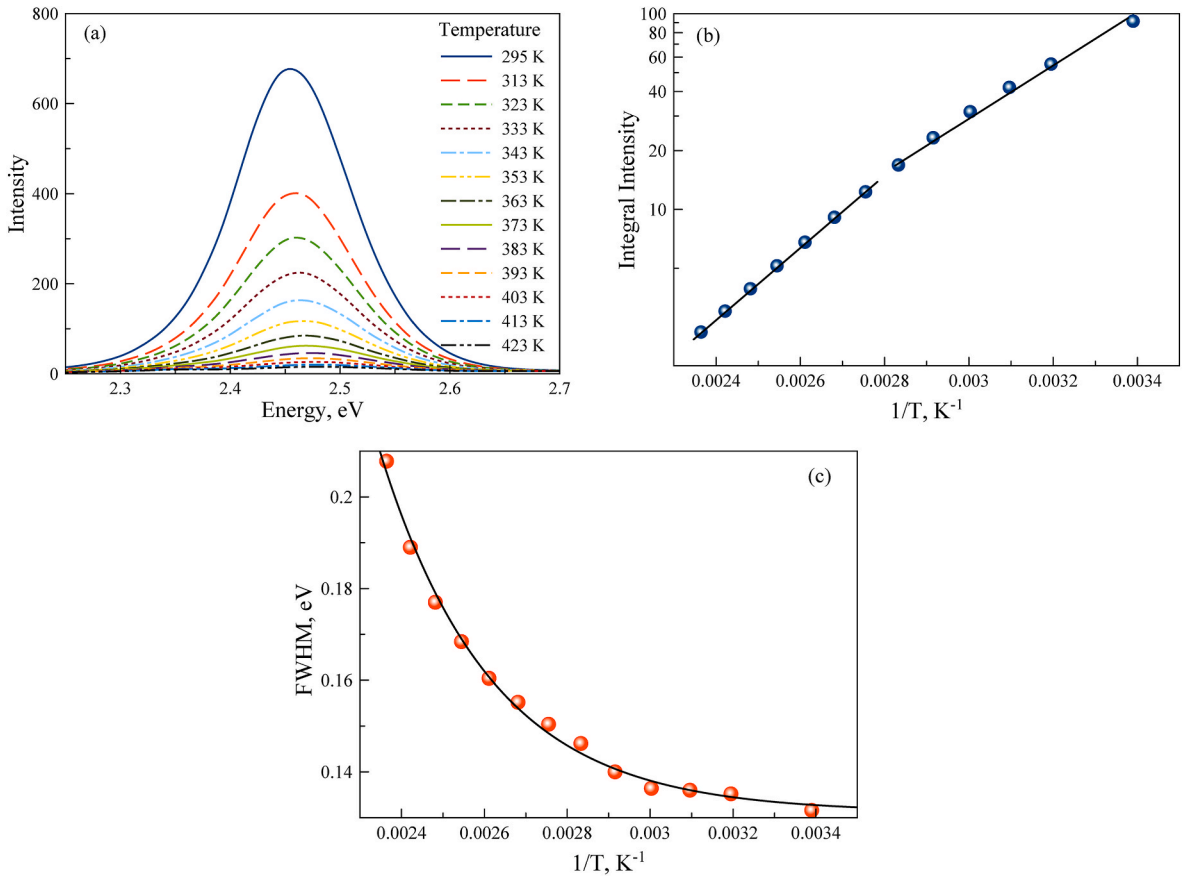

Fig. 3. PL spectra at different temperatures (a) and the dependence of PL integral intensity in logarithmic scale on the inverse temperature (b); and the inverse temperature dependence of PL FWHM (c) for NCs with an average size of 7.5 nm in FP glass during heating from 300 to 423 K.

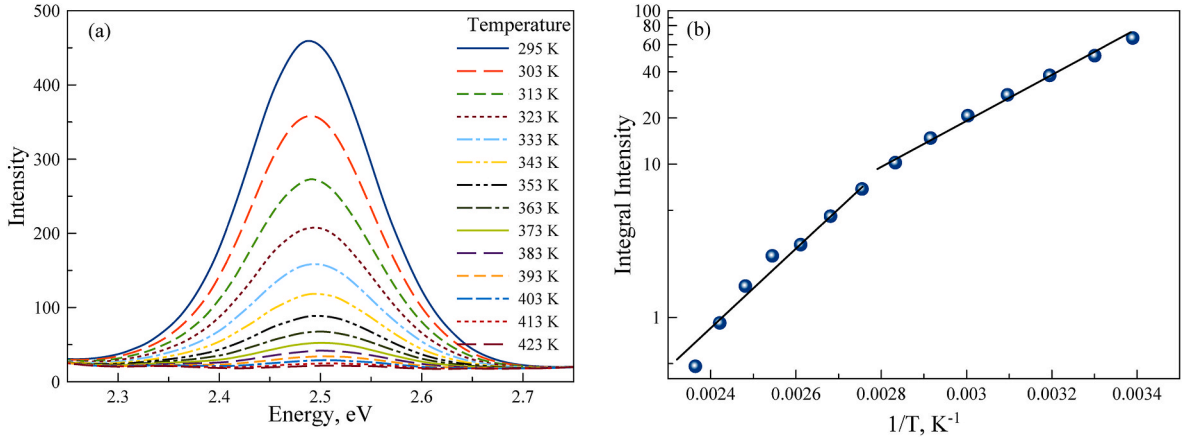

Fig. 4. PL spectra at different temperatures (a) and the dependence of PL integral intensity in logarithmic scale on the inverse temperature (b); for NCs with an average size of 6 nm in FP glass during heating from 300 to 423 K.

nanocrystals to more symmetric state [20].

Figs. 2 and 3(c) shows the inverse temperature dependence of the full-width-half-maxima (FWHM) of the PL band for the samples with NCs size 7.5 and 9 nm. The width of the PL band increase with the temperature rises for the samples with NCs size 7.5 and 9 nm. The FWHM for the sample with NCs size of 6 nm the remains virtually unchanged over the entire temperature range. It is known thermal broadening of PL increases linearly on acoustic phonon–exciton coupling and nonlinearly based on longitudinal optical (LO) phonon–exciton coupling [25]. The nonlinear increase in the PL linewidth with elevated temperature is evidence for the contribution of both acoustic and optical phonons in the thermal broadening.

To prove the validity of the explanation of the PL intensity decreasing above 350 K, it is necessary to analyze the changing of the coefficient of the temperature band gap shift. According to the [21] when the crystal structure changes from orthorhombic to tetragonal phase, there is a sharp increase in the coefficient from 8×10^{-5} to 34×10^{-5} eV K.$^{-1}$

Fig. 5 shows the temperature dependences of the energy position of PL maxima for three samples under study. It was shown [21] that results

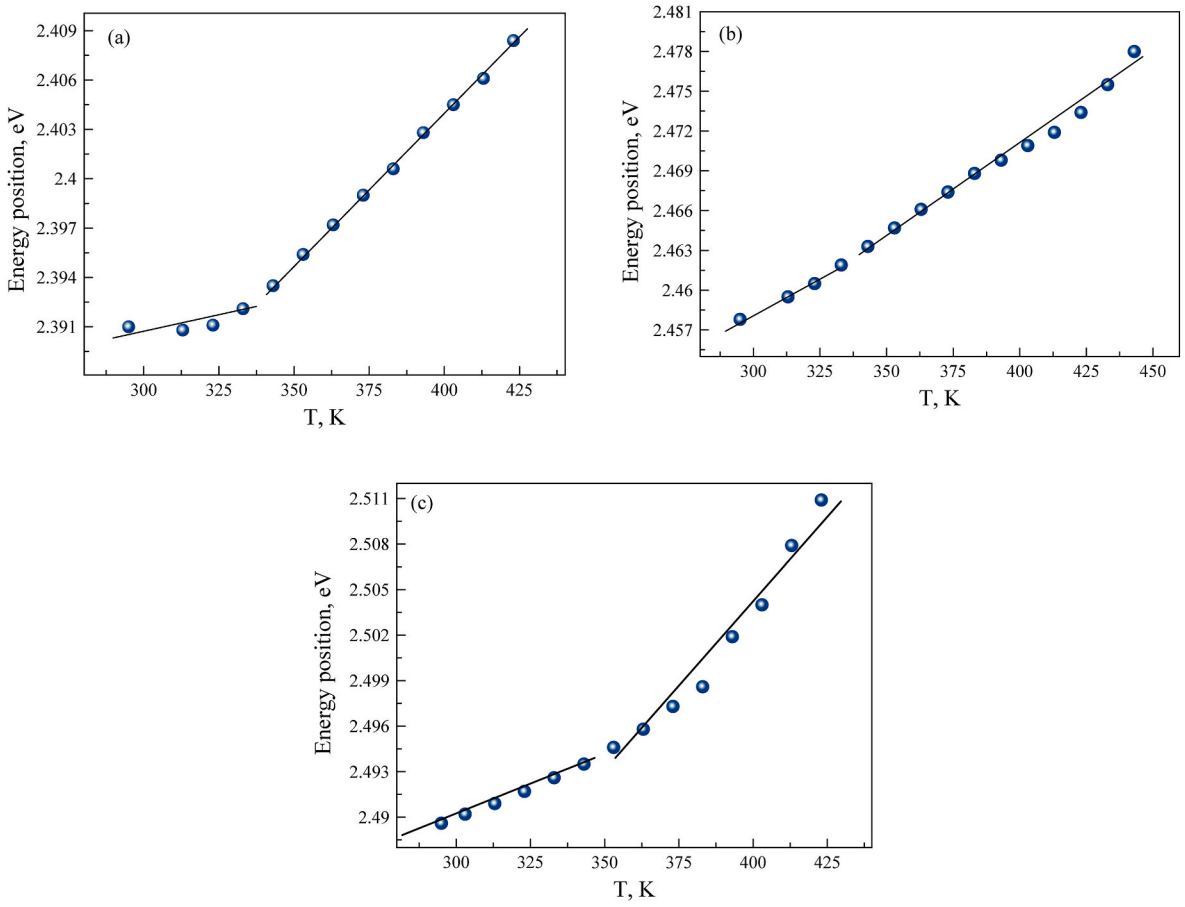

Fig. 5. The temperature dependences of the PL peak energies for $CsPbBr_3$ NCs with sizes 9.0 nm (a), 7.5 nm (b) and 6.0 nm (c).

of the temperature coefficient bandgap energy shift of $CsPbBr_3$ NCs obtained by Tauk fitting of absorption spectra and by energy shift of PL maximum were identical. Linear approximation of the experimental data allows us to make some conclusions. For NCs with sizes ~9 nm at temperatures up to 350 K the shift is small ($dE_g/dT = -0.5 \times 10^{-4}$ eV K^{-1}). As the temperature rises, the shift occurs according to a linear law with $dE_g/dT = -1.72 \times 10^{-4}$ eV K^{-1} (350 423 K) (Fig. 5a). For 7.5 nm sized NCs, the temperature dependence changes at ~350 K and can be described by two straight lines with coefficients $dE_g/dT = -1.2 \times 10^{-4}$ eV K^{-1} (295 340 K) and -1.65×10^{-4} eV K^{-1} (350 423 K) (Fig. 5b). A similar dependence is observed for NCs with a size of 6.0 nm. The shift value changes also at 340–350 K and can be described by two straight lines with coefficients $dE_g/dT = -0.8 \times 10^{-4}$ eV K^{-1} (295–340 K) and -1.4×10^{-4} eV K^{-1} (350 423 K) (Fig. 5c).

Thereby the coefficient dE_g/dT of the NCs with sizes near the Bohr exciton radius has two different slopes at temperature region 295–423 K. In the range of 295–350 K (Fig. 5) the temperature coefficients changes from -0.5 to -1.2×10^{-4} eV K^{-1} for the samples under study. This result is close to the one obtained for orthorhombic $CsPbBr_3$ bulk crystals [21]. When the temperature increases, the slope increases, which also agrees with the data of [21]. However, our data showed values of temperature coefficients changes from -1.4×10^{-4} to -1.7×10^{-4} eV K^{-1} in the temperature range of 350–423 K, which is approximately two times smaller than the previously obtained values for bulk crystals in the same temperature range 350–425 K (3.4×10^{-4} eV K^{-1}). Such a change from the bulk value with decreasing NCs size is characteristic of quantum confinement [36]. The decreasing of the PL intensity could be explained by the transition of nanocrystals to more symmetric phase. It should be noted that our experiment is implemented within the limits of the existence of a monoclinic high-temperature phase [20], the transition to the cubic phase occurs at 403 K [20].

Thus, we can draw conclusions by comparing the data from Figs. 2–4 and 5. The insignificant inflection in the temperature dependencies of NCs with sizes of 9.0 nm in Fig. 5a is in good agreement with a very insignificant inflection in Fig. 2b. Comparison of the integral intensity and shift coefficient dependences (Figs. 3b and 5b) shows the presence of a weak inflection at 340–350 K for NCs with size 7.5 nm. The inflection in the dependences of the glass with NCs of sizes 6 nm, also coincides (350 K), and the changes in the slope are sharper. Thus, the inflection temperatures coincide on the dependences of three sizes of NCs.

The results are the follows:

(i) the coefficient dE_g/dT depends on the size of the NCs. The coefficient value is close to the results obtained for $CsPbBr_3$ bulk crystals up to 350 K and reduced more than 2 times compared to the value of the bulk crystals [21] at higher temperature;
(ii) the acceleration of the decreasing in PL intensity at 350 K indicates the transition of nanocrystals to higher symmetric phase.

Table 1 lists the temperature coefficient of bandgap energy shift for bulk, colloidal NCs and for CsPbBr3 NCs formed in fluorophosphate glasses.

4. Summary

The changes in the $CsPbBr_3$ NCs characteristics (the temperature coefficient of the band gap shift and the decrease of the luminescence intensity) occur at 350 K, which corresponds to a first-order isostructural phase transition in the monoclinic high-temperature phase. The

Table 1
Temperature coefficient of bandgap energy shift for $CsPbBr_3$ semiconductors.

	300-(350–380) K	(380–435 K)	References
$CsPbBr_3$ bulk	$-0.7 \pm 0.1 \times 10^{-4}$ eV K^{-1}	$-3.41 \pm 0.1 \times 10^{-4}$ eV K^{-1}	[21]
$CsPbBr_3$ colloidal NCs with size 11 nm	-0.73×10^{-4} eV K^{-1}	-0.73×10^{-4} eV K^{-1}	[25]
$CsPbBr_3$ NCs in glass, size 9 nm	-0.5×10^{-4} eV K^{-1}	-1.72×10^{-4} eV K^{-1}	This work
$CsPbBr_3$ NCs in glass size 7.5 nm	-1.2×10^{-4} eV K^{-1}	-1.65×10^{-4} eV K^{-1}	This work
$CsPbBr_3$ NCs in glass size 6 nm	-0.8×10^{-4} eV K^{-1}	-1.4×10^{-4} eV K^{-1}	This work

coefficient dE_g/dT depends on the size of the NCs and reduces more than 2 times compared to the values of the bulk crystals. The transition of $CsPbBr_3$ nanocrystals to the more symmetric phase above 350 K decreases luminescence intensity.

Credit author statement

Elena Kolobkova: Conceptualization, Writing – original draft, Funding acquisition. Rawan Semaan: Data curation, Methodology. Maria S. Kuznetsova: Writing – review & editing. Nikolay V. Nikonorov: Supervision, Formal analysis.

Declaration of competing interest

The authors declare that they have no known competing financial interests or personal relationships that could have appeared to influence the work reported in this paper.

Data availability

No data was used for the research described in the article.

Acknowledgements

This research was supported by Priority 2030 Federal Academic Leadership Program, Russia. M.S.K. thanks the St. Petersburg State University Research Grant No 91182694.

References

[[1] L. Protesescu, S. Yakunin, M.I. Bodnarchuk, F. Krieg, R. Caputo, C.H. Hendon, R. X. Yang, A. Walsh, M.V. Kovalenko, Nanocrystals of cesium lead halide perovskites ($CsPbX_3$, X = Cl, Br, and I): novel optoelectronic materials showing bright emission with wide color gamut, Nano Lett. 15 (2015) 3692–3696, https://doi.org/10.1021/nl5048779.

[2] D. Fröhlich, K. Heidrich, H. Künzel, G. Trendel, J. Treusch, Cesium-trihalogen-plumbates a new class of ionic semiconductors, J. Lumin. 18–19 (1979) 385–388, https://doi.org/10.1016/0022-2313(79)90146-7.

[3] S. Yakunin, L. Protesescu, F. Krieg, M.I. Bodnarchuk, G. Nedelcu, M. Humer, G. De Luca, M. Fiebig, W. Heiss, M.V. Kovalenko, Low-threshold amplified spontaneous emission and lasing from colloidal nanocrystals of cesium lead halide perovskites, Nat. Commun. 6 (2015) 1–9, https://doi.org/10.1038/ncomms9056.

[4] Y. Wang, X. Li, J. Song, L. Xiao, H. Zeng, H. Sun, All-Inorganic colloidal perovskite quantum dots: a new class of lasing materials with favorable characteristics, Adv. Mater. 27 (2015) 7101–7108, https://doi.org/10.1002/adma.201503573.

[5] X. Li, Y. Wu, S. Zhang, B. Cai, Y. Gu, J. Song, H. Zeng, $CsPbX_3$ quantum dots for lighting and displays: room-temperature synthesis, photoluminescence superiorities, underlying origins and white light-emitting diodes, Adv. Funct. Mater. 26 (2016) 2435–2445, https://doi.org/10.1002/adfm.201600109.

[6] X. Zhang, C. Sun, Y. Zhang, H. Wu, C. Ji, Y. Chuai, P. Wang, S. Wen, C. Zhang, W. W. Yu, Bright perovskite nanocrystal films for efficient light-emitting devices, J. Phys. Chem. Lett. 7 (2016) 4602–4610, https://doi.org/10.1021/acs.jpclett.6b02073.

[7] G. Li, H. Wang, T. Zhang, L. Mi, Y. Zhang, Z. Zhang, W. Zhang, Y. Jiang, Solvent-polarity-engineered controllable synthesis of highly fluorescent cesium lead halide perovskite quantum dots and their use in white light-emitting diodes, Adv. Funct. Mater. 26 (2016) 8478–8486, https://doi.org/10.1002/adfm.201603734.

[8] E. Yassitepe, Z. Yang, O. Voznyy, Y. Kim, G. Walters, J.A. Castañeda, P. Kanjanaboos, M. Yuan, X. Gong, F. Fan, J. Pan, S. Hoogland, R. Comin, O. M. Bakr, L.A. Padilha, A.F. Nogueira, E.H. Sargent, E. Yang, Z. Voznyy, O. Kim, Y. Walters, G.A. Castañeda, J.A. Kanjanaboos, P. Yuan, M. Gong, X. Fan, F. Pan, J. Hoogland, S. Comin, R. Bakr, O.M. Padilha, L.A. Nogueira, A.F. Sargent, Amine-free synthesis of cesium perovskite, Adv. Funct. Mater. 26 (2016) 8757, https://doi.org/10.1002/adfm.201604580.

[9] J. Song, J. Li, X. Li, L. Xu, Y. Dong, H. Zeng, Quantum dot light-emitting diodes based on inorganic perovskite cesium lead halides ($CsPbX_3$), Adv. Mater. 27 (2015) 7162–7167, https://doi.org/10.1002/adma.201502567.

[10] M. Meyns, M. Perálvarez, A. Heuer-Jungemann, W. Hertog, M. Ibáñez, R. Nafria, A. Genç, J. Arbiol, M.V. Kovalenko, J. Carreras, A. Cabot, A.G. Kanaras, Polymer-enhanced stability of inorganic perovskite nanocrystals and their application in color conversion LEDs, ACS Appl. Mater. Interfaces 8 (2016) 19579–19586, https://doi.org/10.1021/acsami.6b02529.

[11] Q. Zhou, Z. Bai, W. Lu, Y. Wang, B. Zou, H. Zhong, In situ fabrication of halide perovskite nanocrystal-embedded polymer composite films with enhanced photoluminescence for display backlights, Adv. Mater. 28 (2016) 9163–9168, https://doi.org/10.1002/adma.201602651.

[12] C. Sun, Y. Zhang, C. Ruan, C. Yin, X. Wang, Y. Wang, W.W. Yu, Efficient and stable white LEDs with silica-coated inorganic perovskite quantum dots, Adv. Mater. 28 (2016) 10088–10094, https://doi.org/10.1002/adma.201603081.

[13] R.E. Brandt, J.R. Poindexter, P. Gorai, R.C. Kurchin, R.L.Z. Hoye, L. Nienhaus, M. W.B. Wilson, J.A. Polizzotti, R. Sereika, R. Zaltauskas, L.C. Lee, J.L. MacManus-Drisco, M. Bawendi, V. Stevanovic, T. Buonassisi, Searching for "defect-tolerant" photovoltaic materials: combined theoretical and experimental screening, Chem. Mater. 29 (2017) 4667–4674, https://doi.org/10.1021/acs.chemmater.6b05496.

[14] S. Liu, Y. Luo, M. He, X. Liang, W. Xiang, Novel CsPbI3 QDs glass with chemical stability and optical properties, J. Eur. Ceram. Soc. 38 (2018) 1998–2004, https://doi.org/10.1016/j.jeurceramsoc.2017.10.012.

[15] S. Liu, M. He, X. Di, P. Li, W. Xiang, X. Liang, Precipitation and tunable emission of cesium lead halide perovskites ($CsPbX_3$, X = Br, I) QDs in borosilicate glass, Ceram. Int. 44 (2018) 4496–4499, https://doi.org/10.1016/j. ceramint.2017.12.012.

[16] P. Li, C. Hu, L. Zhou, J. Jiang, Y. Cheng, M. He, X. Liang, W. Xiang, Novel synthesis and optical characterization of CsPb2Br5 quantum dots in borosilicate glasses, Mater. Lett. 209 (2017) 483–485, https://doi.org/10.1016/j. matlet.2017.08.079.

[17] Y. Ye, W. Zhang, Z. Zhao, J. Wang, C. Liu, Z. Deng, X. Zhao, J. Han, Highly luminescent cesium lead halide perovskite nanocrystals stabilized in glasses for light-emitting applications, Adv. Opt. Mater. 7 (2019), 1801663, https://doi.org/10.1002/adom.201801663.

[18] S. Liu, M. He, X. Di, P. Li, W. Xiang, X. Liang, Precipitation and tunable emission of cesium lead halide perovskites ($CsPbX_3$, X = Br, I) QDs in borosilicate glass, Ceram. Int. 44 (2018) 4496–4499, https://doi.org/10.1016/j. ceramint.2017.12.012.

[19] B. Ai, C. Liu, Z. Deng, J. Wang, J. Han, X. Zhao, Low temperature photoluminescence properties of $CsPbBr_3$ quantum dots embedded in glasses, Phys. Chem. Chem. Phys. 19 (2017) 17349–17355, https://doi.org/10.1039/c7cp02482g.

[20] S.Z. Liu, A.R. DeFilippo, M. Balasubramanian, Z.X. Liu, S.G. Wang, Y. Chen, S. Chariton, V. Prakapenka, X.P. Luo, L.Y. Zhao, J. San Martin, Y.X. Lin, Y. Yan, S. K. Ghose, T.A. Tyson, High-resolution in-situ synchrotron X-ray studies of inorganic perovskite CsPbBr3: new symmetry assignments and structural phase transitions, Adv. Sci. 8 (18) (2021), 2003046, https://doi.org/10.1002/advs.202003046.

[21] G. Mannino, I. Deretzis, E. Smecca, A. La Magna, A. Alberti, D. Ceratti, D. Cahen, Temperature-dependent optical band gap in $CsPbBr_3$, $MAPbBr_3$, and $FAPbBr_3$ single crystals, J. Phys. Chem. Lett. 11 (2020) 2490, https://doi.org/10.1021/acs.jpclett.0c00295.

[22] J. Li, X. Yuan, P. Jing, J. Li, M. Wei, J. Hua, J. Zhao, L. Tian, Temperature-dependent photoluminescence of inorganic perovskite nanocrystal films, RSC Adv. 6 (82) (2016) 78311–78316, https://doi.org/10.1039/c6ra17008k.

[23] B.T. Diroll, H. Zhou, R.D. Schaller, Low-temperature absorption, photoluminescence, and lifetime of $CsPbX_3$ (X = Cl, Br, I) nanocrystals, Adv. Funct. Mater. 28 (2018), 1800945, https://doi.org/10.1002/adfm.201800945.

[24] R. Saran, A. Heuer-Jungemann, A.G. Kanaras, R.J. Curry, Giant bandgap renormalization and Exciton−Phonon scattering in perovskite nanocrystals, Adv. Opt. Mater. 5 (17) (2017), 1700231, https://doi.org/10.1002/adom.201700231.

[25] B.T. Diroll, G. Nedelcu, M.V. Kovalenko, R.D. Schaller, High-temperature photoluminescence of $CsPbX_3$ (X = Cl, Br, I) nanocrystals, Adv. Funct. Mater. 27 (2017), 1606750, https://doi.org/10.1002/adfm.201606750.

[26] M.S. Kirschner, B.T. Diroll, P. Guo, S.M. Harvey, W. Helweh, N.C. Flanders, A. Brumberg, N.E. Watkins, A.l A. Leonard, A.M. Evans, M.R. Wasielewski, W. R. Dichtel, X. Zhang, L.X. Chen, R. D. Schaller Photoinduced, Reversible phase transitions in all-inorganic perovskite nanocrystals, Nat. Commun. 10 (2019) 504, https://doi.org/10.1038/s41467-019-08362-3|www.nature.com/naturecommunications.

[27] A. Swarnkar, R. Chulliyil, V.K. Ravi, M. Irfanullah, A. Chowdhury, A. Nag, Colloidal CsPbBr3 perovskite nanocrystals: luminescence beyond traditional quantum dots, Angew. Chem. Int. Ed. 54 (2015), 15424, https://doi.org/10.1002/anie.201508276.

[28] K. Wei, Z. Xu, R. Chen, X. Zheng, X. Cheng, T. Jiang, Temperature-dependent excitonic photoluminescence excited by two photon absorption in perovskite $CsPbBr_3$ quantum dots, Opt. Lett. 41 (16) (2016) 3821–3824, https://doi.org/10.1364/OL.41.003821 [25.

[29] B. Vaynberg, M. Matusovsky, M. Rosenbluh, E. Kolobkova, A. Lipovskii, High optical nonlinearity of CdSxSe1 - X microcrystals in fluorine-phosphate glass, Opt Commun. 132 (1996) 307–310, https://doi.org/10.1016/0030-4018(96)00373-2.

[30] E.V. Kolobkova, A.A. Lipovskii, V.D. Petrikov, V.G. Melekhin, Fluorophosphate glasses with quantum dots based on lead sulfide, Glas, Phys. Chem. 28 (2002) 251–255, https://doi.org/10.1023/A:1019918530283.
[31] M.S. Kuznetsova, R.V. Cherbunin, V.M. Litvyak, E.V. Kolobkova, Spectroscopy of PbS and PbSe Quantum Dots in Fluorine Phosphate Glasses, Semiconductors 52 (2018) 558–561, https://doi.org/10.1134/S1063782618050172.
[32] E.V. Kolobkova, M.S. Kuznetsova, N.V. Nikonorov, Perovskite CsPbX3 (X=Cl, Br, I) nanocrystals in fluorophosphate glasses, NonCryst. Sol. 563 (2021), 120811. DOI. org/10.1016/j.jnoncrysol.2021.12081X.
[33] Luo, R. Lai, Y. Li, Y. Han, G. Liang, X. Liu, T. Ding, J. Wang, K. Wu, Triplet energy transfer from CsPbBr3 nanocrystals enabled by quantum confinement, J. Am. Chem. Soc. 141 (2019) 4186–4190, https://doi.org/10.1021/jacs.8b13180.
[34] H. Shi, M.-H. Du, Shallow halogen vacancies in halide optoelectronic materials, Phys. Rev. B 90 (2014) 174103A, https://doi.org/10.1103/PhysRevB.90.174103.
[35] M. Sebastian, J.A. Peters, C.C. Stoumpos, J. Im, S.S. Kostina, Z. Liu, M. G. Kanatzidis, A.J. Freeman, B.W. Wessels, Excitonic emissions and above-band-gap luminescence in the single-crystal perovskite semiconductors CsPbBr3 and CsPbCl3, Phys. Rev. B 92 (2015), 235210, https://doi.org/10.1103/PhysRevB.92.235210.
[36] Olkhovets, R.C. Hsu, A. Lipovskii, F.W. Wise, Size-dependent temperature variation of the energy gap in lead-salt quantum dots, Phys. Rev. Lett. 81 (1998) 3539–3542, https://doi.org/10.1103/PhysRevLett.81.3539.